Nanoscale

Accepted Manuscript

This article can be cited before page numbers have been issued, to do this please use: I. G. Theodorou, P. Ruenraroengsak, D. Gonzalez Carter, Q. Jiang, E. Yagüe, E. O. Aboagye, C. R. Coombes, A. E. Porter, M. P. Ryan and F. Xie, *Nanoscale*, 2019, DOI: 10.1039/C8NR09409H.

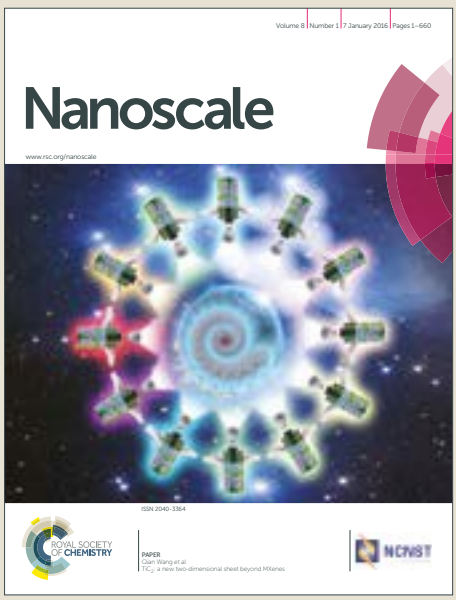

ROYAL SOCIETY OF CHEMISTRY

rsc.li/nanoscale

DOI: 10.1039/C8NR09409H

Towards Multiplexed Near-Infrared Cellular Imaging using Gold Nanostar Arrays with Tunable Fluorescence Enhancement

Ioannis G. Theodorou[1, 2], Pakatip Ruenraroengsak[1, 3], Daniel Gonzalez Carter[1, 4], Qianfan Jiang[1], Ernesto Yagüe[5], Eric O. Aboagye[5], R. Charles Coombes[5], Alexandra E. Porter[1], Mary P. Ryan[1] and Fang Xie[1,*]

[1]Department of Materials and London Centre for Nanotechnology, Imperial College London, Exhibition Road, London SW7 2AZ, United Kingdom

[2]Cancer Biophysics Laboratory, Department of Mechanical and Manufacturing Engineering, University of Cyprus, 40 Macedonias Avenue, Latsia 2238, Cyprus

[3]Faculty of Pharmacy, Mahidol University, 447 Sri-Ayuthaya Rajathevi, Bangkok 10400, Thailand

[4]Innovation Center of NanoMedicine, Kawasaki Institute of Industrial Promotion, 3-25-14 Tonomachi, Kawasaki, Japan

[5]Department of Surgery and Cancer, Imperial College London, Du Cane Road, London W12 0NN, United Kingdom

*E-mail: f.xie@imperial.ac.uk

KEYWORDS: gold nanostars; plasmonic arrays; near infrared; imaging; fluorescence enhancement.

Abstract: Sensitive detection of disease biomarkers expressed by human cells is critical to the development of novel diagnostic and therapeutic methods. Here we report that plasmonic arrays based on gold nanostar (AuNS) monolayers enable up to 19-fold fluorescence enhancement for cellular imaging in the near-infrared (NIR) biological window, allowing the application of low quantum yield fluorophores for sensitive cellular imaging. The high fluorescence enhancement together with low autofluorescence interference in this wavelength range enable higher signal-to-noise ratio compared to other diagnostic modalities. Using AuNSs of different geometries and therefore controllable electric field enhancement, cellular imaging with tunable enhancement factors is achieved, which may be useful for the development of multicolour and multiplexed platforms for a panel of biomarkers, allowing to

distinguish different subcell populations at the single cell level. Finally, the uptake of AuNS within HeLa cells and their high biocompatibility, pave the way for novel high-performance *in vitro* and *in vivo* diagnostic platforms.

Introduction

Fluorescence labelling and imaging are among the most advanced techniques for non-invasive and non-destructive visualization of biological tissues and processes. In particular, sensitive detection and analysis of various disease biomarkers expressed both on the cell surface and intracellularly, is essential for elucidating cell-signalling pathways and developing novel diagnostic and therapeutic methods. Despite widespread application of fluorescence cell labelling in clinical practice, a plateau in the technology has been reached because of the high light absorption by water and blood in the visible wavelength range.[1] Recently, fluorophores emitting in the near-infrared (NIR; 650-900 nm) and second near-infrared (NIR-II; 1.0−1.7 μm) windows, have attracted particular interest,[2-4] because low absorption of light by water and haemoglobin allows high transparency for tissue imaging.[5] Meanwhile, low autofluorescence from organic molecules enables higher signal-to-noise ratio compared to the visible range.[6] In addition, diminished photon scattering allows higher tissue penetration in the NIR-II window. However, the low quantum yields (QY) of NIR/NIR-II fluorophores, coupled with reduced quantum efficiencies of detectors/cameras in this wavelength range, have so far limited the sensitivity and dynamic range of NIR detection. Improvement in the signal-to-noise ratios in the NIR would enable multicolour detection of cellular biomarkers over the broadest possible wavelength range. Therefore, novel approaches for sensitive detection of cellular proteins and biomarkers in the NIR windows are urgently required.

Research efforts have recently focused on metal enhanced fluorescence (MEF), an optical process in which the near-field interaction of fluorophores with metallic nanoparticles could, under specific conditions, produce large fluorescence enhancements.[1, 7-10] This light amplification can be exploited to considerably increase detection sensitivity, therefore improving the performance of fluorescence-based technologies.[1] To date, a limited number of platforms allowing NIR fluorescence enhancement have been reported.[11-13] In our own work, arrays of Ag or Au nanotriangles/nanodiscs with tunable optical features obtained by nanosphere

View Article Online
DOI: 10.1039/C8NR09409H

lithography, allowed up to two orders of magnitude NIR fluorescence enhancement.[9, 11] In addition, plasmonic gold nano-island films have attracted attention for several applications of NIR fluorescence-enhanced detection,[14, 15] and have recently been applied for enhancing the imaging of fluorescently labelled biomarkers on cells.[16] However, systematic localized surface plasmon resonance (LSPR) tuning of these Au island films was not possible.[17] In contrast, for spiky gold nanostars (AuNSs), the LSPR peak position is tunable based on their size and shape, as well as the length and aspect ratio of the spikes.[18, 19] Using self-assembled AuNS substrates, we have recently measured over 320 times fluorescence enhancement in the NIR region, as well as up to 50-fold enhancement factors in the NIR-II region, for NIR/NIR-II dye monolayers incorporated on to the AuNS substrates.[20] By manipulating the electric field enhancement of AuNSs through control of their morphological features, we were able to control the magnitude of excitation enhancement and thus the overall enhancement factors.[20] However, the capabilities of these AuNS substrates for fluorescence-enhanced cellular imaging have not been previously tested.

In the present work, we present sensitive and tunable imaging of NIR-labelled HeLa cells on plasmonic AuNS arrays. HeLa cells are a cervical cancer cell line that overexpresses the Folate Receptor alpha (FRα), and were used as a model for FRα labelling.[21] FRa is a receptor known to be overexpressed on the surface of several types of human cancer cells, and has attracted significant interest for cancer cell targeting.[22] As a control, we employed MCF-7 cells, an estrogen receptor positive (ER+) breast cancer cell line that is FRα-negative.[21] To obtain arrays with tunable plasmonic properties, two types of AuNSs with different morphological features and LSPR responses are used. First, the two types of AuNS arrays were used to quantify the fluorescence enhancement of NIR dye molecules positioned in proximity to the AuNS surface, prior to using these fluorophores for cell labelling (Figure 1a). Therefore, the fluorescence enhancement of Alexa Fluor® 680 (AF680; Abs 679 nm/Em 702 nm) was measured by incorporating AF680 dye monolayers on to the AuNS array surface. Along our previous findings for monolayers of other NIR/NIR-II fluorophores immobilized on AuNS substrates,[20] the significant fluorescence enhancement of up to 147 times for AF680 monolayers measured here, confirms that AuNS arrays are promising NIR-MEF platforms for biosensing applications over a wide wavelength range in the NIR windows. Then, the AuNS arrays were used for fluorescence-enhanced cell imaging experiments, as illustrated schematically in

View Article Online
DOI: 10.1039/C8NR09409H

Figure 1b. Following FRα labelling on the cell surface with AF680 (Figure 1vi-viii), the two types of AuNS arrays allow fluorescence enhanced cellular imaging with tunable enhancement factors and up to 19 times higher mean fluorescence intensity for AF680-labelled cells. Finally, the uptake of colloidal AuNSs and their biocompatibility with HeLa cells, demonstrate that AuNSs are suitable for live cell imaging and pave the way towards developing further *in vivo* applications.

Experimental

Materials

Gold chloride trihydrate ($HAuCl_4.3H_2O$), sodium citrate tribasic dehydrate, silver nitrate ($AgNO_3$), L-ascorbic acid (AA), hydrogen peroxide solution (H_2O_2, 30 wt. %), (3-Mercaptopropyl)trimethoxysilane (MPTMS, 95%), phosphate buffered saline (PBS, pH 7.4), DMEM tissue culture medium and biotinylated bovine serum albumin (bBSA) were purchased from Sigma-Aldrich, UK. Glass microscope slides, hydrochloric acid (HCl, 37%), sulphuric acid (H_2SO_4, 96%), acetone and 2-propanol were obtained from VWR International, UK. Streptavidin conjugated AlexaFluor® 680 (AF680), 4',6-Diamidino-2-Phenylindole Dihydrochloride (DAPI), Folate Receptor alpha Polyclonal Antibody and Alexa Fluor 680-labelled Donkey anti-Sheep IgG (H+L) Cross-Adsorbed Secondary Antibody were purchased from ThermoFischer Scientific. De-ionized (DI) water purified using the Millipore Milli-Q gradient system (>18.2 MΩ) was used in all the experiments.

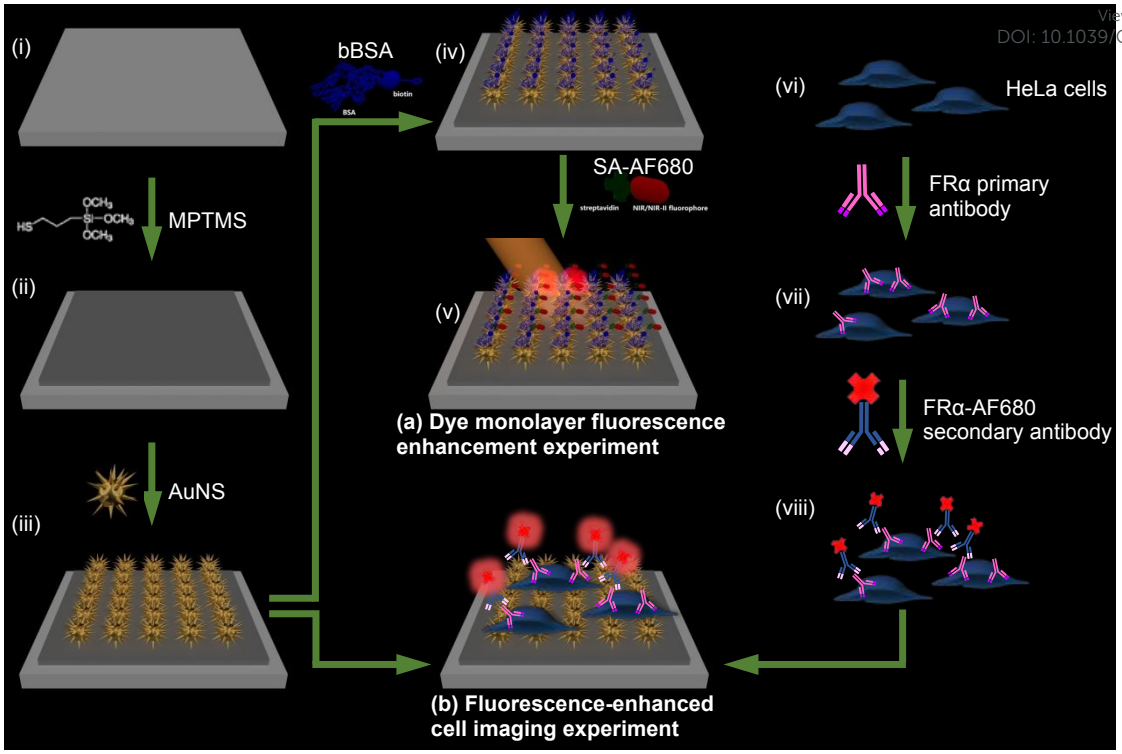

Figure 1. Schematic workflow of gold nanostar (AuNS) substrate preparation and experimental steps for dye-monolayer fluorescence enhancement experiments (a) and fluorescence-enhanced cell imaging experiments (b). Clean glass slides (i) were coated with (mercaptopropyl)trimethoxysilane (MPTMS) (ii) and used for the fabrication of AuNS self-assembled monolayers through thiolate−gold coordinative bonding (iii). For experiment (a), biotinylated bovine serum albumin (bBSA) self-assembled monolayers were deposited on AuNS substrates (iv), followed by immobilization of streptavidin-functionalized AlexaFluor 680 (SA-AF680) fluorophore monolayers onto the substrates through biotin−avidin binding (v). For experiment (b), HeLa cells (vi) were labelled with Folate Receptor alpha (FRα) Polyclonal Antibody (vii), and counterstained with AlexaFluor 680-conjugated (Frα-AF680) Secondary Antibody (viii). The labelled cells were adsorbed on to AuNS substrates for fluorescence imaging.

Experimental workflow

A schematic workflow of AuNS substrate preparation and of the experimental steps followed in this work is presented in Figure 1.

For AuNS substrate preparation, AuNSs of two different sizes were first synthesized as described in detail in the section “Synthesis of AuNSs”. Then, clean glass microscope slides (Figure 1i) were silanized (“Preparation of MPTMS@Glass

View Article Online
DOI: 10.1039/C8NR09409H

slides"; Figure 1ii), and used to assemble the plasmonic AuNS arrays ("Formation of AuNS self-assembled monolayers on MPTMS@Glass slides"; Figure 1iii).

To quantify the fluorescence enhancement of AF680 resulting from the AuNS arrays (Figure 1a), dye monolayers were formed as explained in the section "Immobilization of fluorophore–protein conjugation monolayers", by first coating the substrates with biotinylated bovine serum albumin (bBSA; Figure 1iv) and then immobilizing streptavidin-functionalized AF680 (Figure 1v) on the substrate surface. The quantification of fluorescence enhancement is outlined in section "Fluorescence measurements and analysis".

For fluorescence-enhanced cell imaging experiments ("Cell Labelling and imaging"; Figure 1b), HeLa cells ("Cell Culture"; Figure 1vi) were labelled with Folate Receptor alpha (FRα) Polyclonal Antibody (Figure 1vii), and counterstained with AF680-conjugated (Frα-AF680) Secondary Antibody (Figure 1viii). Then, labelled cells were adsorbed on the AuNS arrays (Figure 1iii) for fluorescence imaging.

Synthesis of AuNSs

Surfactant-free synthesis of gold nanostars (AuNS) of two different sizes, referred to as small (S-AuNS) and large (L-AuNS) gold nanostars, was carried out as described in our previous work[20] *via* a seed mediated two-step protocol.[19] By avoiding toxic or hard to remove surfactants, like cetyltrimethylammonium bromide/chloride (CTAB/CTAC), the AuNSs are highly biocompatible and can be easily functionalized for further development of *in vivo* imaging applications. Briefly, spherical citrate-stabilized Au nanoparticle (AuNP) seeds, with average sizes of 15 nm ($AuNP_{15}$) and 50 nm ($AuNP_{50}$), were prepared by heating 100 mL of a 0.25 mM aqueous $HAuCl_4 \cdot 3H_2O$ solution in a 250 mL Erlenmeyer flask, under magnetic stirring. Once the solution reached boiling point, 1 or 0.25 mL of a 3.3% (w/v) aqueous sodium citrate solution were rapidly added, under vigorous stirring. Colour started appearing in the solution after 1-3 min, and heating was continued until it became a stable bright red colour (within 10 min). The solution was then cooled in an ice bath, its volume was made up to 100 mL with Milli-Q water, and it was stored at 4°C.

For S-AuNS synthesis, 200 µL of $AuNP_{15}$ were added to 10 mL of 0.1 mM $HAuCl_4 \cdot 3H_2O$ with 10 µL of 1 M HCl in a 30 mL glass vial at room temperature, under moderate stirring. In the case of L-AuNS, 300 µL of $AuNP_{50}$ were added to 10

mL of 0.3 mM $HAuCl_4 \cdot 3H_2O$, containing 10 μL of 1 M HCl. Then, 150 μL of 2 mM $AgNO_3$ and 50 μL of 100 mM AA were quickly added. The colour of the solution changed from faint red to blue-green as soon as the AA was added, and stirring was stopped after 30 s. The optical properties of the as-synthesized AuNPs and AuNS were characterized by optical absorption spectroscopy, using an Agilent Cary 5000 UV-Vis-NIR spectrophotometer. Extinction spectra were collected using glass cuvettes from Hellma® Analytics, and both a 100% transmittance (T) and 0% T baseline correction was applied to the data. The 100% T baseline correction was performed using Milli-Q water, to account for water/cuvette absorption.

For preparation of AuNS self-assembled monolayers on silanized glass slides, AuNS were used as-synthesized. For cell uptake and viability experiments, AuNSs were PEGylated by adding mPEG-SH to as-synthesized AuNS solutions. The mixtures were stirred at room temperature for 2 h, washed 2x with DI water by centrifugation at 2000 *g* for 20 min at 4°C, and redispersed in DI water.

Preparation of MPTMS@Glass slides

Silanization of glass slides was performed following a previously described procedure.[19, 23] First, 10 mm × 12 mm pieces of glass microscopes slides were cleaned by successive ultrasonication in acetone, Milli-Q water and 2-propanol, for 10 min each. The slides were dried under a N_2 stream and treated with piranha solution (3:1 v/v H_2SO_4 96%:H_2O_2 30%) for 30 min. Then, they were washed 3 times by ultrasonication in Milli-Q water, for 3 min each. The washed slides were dried in an oven at 140 °C for 1 h, and allowed to cool to room temperature. Then, inside a glass container that had undergone the same cleaning procedure, the slides were immersed in a 5% v/v solution of MPTMS in ethanol, sealed and allowed to react for 4 h in a water bath at 40 °C. After 4 h, the MPTMS solution was discarded and the slides were washed 3 times by ultrasonication in ethanol, for 3 min each. Finally the slides were dried under a N_2 stream and cured in an oven at 100°C for 15 min.

Formation of AuNS self-assembled monolayers on MPTMS@Glass slides

To form AuNS self-assembled monolayers (SAMs), the MPTMS-modified glass slides were placed in glass containers, which had been cleaned with piranha solution as described in the previous section, and immersed in solutions of freshly synthesized AuNS. The containers with the glass slides were sealed and placed on an

View Article Online
DOI: 10.1039/C8NR09409H

orbital shaker (100 rpm), in the dark for 18 h. The AuNS-coated glass slides were rinsed with Milli-Q water 3 times and gently dried under a N_2 stream. All substrates were stored in an evacuate desiccator and used within 1 week of their fabrication.

The morphology of the substrates was examined by field emission gun (FEG) scanning electron microscopy (SEM) using a LEO Gemini 1525 (Carl Zeiss Microscopy GmbH, UK). The SEM was operated in secondary electron mode at an accelerating voltage of 5 kV, using the InLens detector. Their optical properties were measured with an Agilent Cary 5000 UV-Vis-NIR spectrophotometer, using bare glass slides for the 100% transmittance (T) baseline correction.

Immobilization of fluorophore–protein conjugation monolayers

For fluorescence enhancement measurements, as well as cell labelling and imaging, a near-infrared AlexaFluor® dye was used because it is more hydrophobic, photostable and bright, but less pH-sensitive, compared to other commercially available dyes with similar spectral properties, making it more suitable for cell and tissue labelling.[24] Specifically, the Alexa Fluor® 680 (AF680) dye (Abs 679 nm/Em 702 nm) was selected for compatibility with our cell imaging system.

For fluorescence enhancement measurements, the AuNS SAMs and clean glass substrates, as a control, were covered by fluorophore monolayers *via* biotin-streptavidin interaction, as previously described.[7, 20] First, bBSA monolayers were formed on the substrates, by adding 26 μL of a 100 mg/mL bBSA solution in PBS (pH 7.2) to their surface, and incubating for 1 h in a humidified chamber. Binding of the streptavidin–conjugated AF680 to bBSA was achieved by adding 37 μL of a 25 μg/mL fluorophore solution onto the substrate surfaces and incubating for 2 h in humidified chambers in the dark. The substrates were rinsed several times with PBS to remove unbound fluorophores and gently dried under a N_2 stream. Their fluorescence spectra were collected immediately. Clean glass substrates incubated with bBSA only, were used to establish the fluorescence background used as reference.

Fluorescence measurements and analysis

Fluorescence emission spectra of AF680 were collected using a Fluorolog Tau 3 system (Horiba Scientific) with a 450 W Xenon excitation lamp. AF680 was excited at 670 nm, using a 4 nm slit. Fluorescence emission was measured in the range of

View Article Online
DOI: 10.1039/C8NR09409H

690-750 nm using a 5 nm slit. For all samples, the angle of acquisition was set at 30° for accuracy and consistency of the measurements. The fluorescence spectra were averaged over 3 individual spots on each substrate, and over 3 different substrates.

Cell Culture

HeLa and MCF-7 cells were cultured in Dulbecco's Modified Eagle Medium supplemented with 100U/100U/2 mM of Penicillin/Streptomycin/L-Glutamin (PSG; Invitrogen, UK) and 10% newborn calf serum (Invitrogen, UK). The cell lines were maintained in a 37 °C incubator with 5% (v/v) CO_2. Experiments were performed with cultures at 60%-70% confluency.

Cell Labelling and imaging

Culture dishes were washed with PBS, trypsinized (0.25% trypsin, 5 min at room temperature) and cells collected. Cells were washed with fresh tissue culture medium and fixed with 2% PFA for 10 min at room temperature with agitation. The number of fixed cells was counted with a hemocytometer and ≈100 000 cells were labelled with 15 µg/mL Folate Receptor alpha Polyclonal Antibody (ThermoFisher Scientific, PA5-47884) in 5% BSA for 2 h with agitation. Primary antibody-labelled cells were washed three times with PBS and further labelled with 5 µg/mL AlexaFluor 680-conjugated Donkey anti-Sheep IgG Cross-Adsorbed Secondary Antibody (ThermoFisher Scientific, A-21102) in 5% BSA for 2 h with agitation. Following secondary antibody labelling, cells were washed three times with PBS, resuspended in PBS and ~10000 cells adsorbed on to AuNS substrates or bare glass slides overnight at 37 °C in an incubator. After overnight incubation, cells were incubated with DAPI for 10 min at room temperature to stain cell nuclei. DAPI (Abs 358 nm/Em 461 nm) was not used to quantify fluorescence enhancement, as its spectral properties do not overlap with the extinction of AuNS substrates, but only to stain cell nuclei, in order to be able to associate AF680 emission during imaging to the presence of cells. Cells were washed with DI water, dried and preserved on sealed plastic containers at 4 °C before analysis. Cell imaging was performed with a Leica SP5 MP (Leica, Germany) inverted confocal microscope, using a 20x objective (air immersion). Z-stack images comprising the majority of the cell height were collected for the labelled cells. Fluorescence intensities in these images were measured using ImageJ (Fiji) analysis software, by first creating total intensity (SUM) z-projections. Regions of interest

(ROI) surrounding individual cells were selected with the freehand tool, using the DAPI signal as reference. Total cell fluorescence was calculated by measuring the Integrated Density of these ROI, and subtracting the mean background fluorescence from regions with no cells. The background-corrected data were expressed as mean fluorescent intensity (MFI) ± standard deviation (SD). Fluorescence intensities were quantified for forty individual cells per sample using three independent samples per condition.

Cell viability assay

The MTS (3-(4,5-dimethylthiazol-2-yl)-5-(3- carboxymethoxyphenyl)-2-(4-sulfophenyl)-2H–tetrazolium) assay was used to quantify metabolic activity as a parameter of AuNS biocompatibility. HeLa cells were grown in 96-well plates (3000 cells/well). Before cell treatment, AuNSs were diluted in complete medium and ultrasonicated for 1 min at RT. Immediately after sonication, HeLa cells were exposed to the AuNS at concentrations 0-25 μg/mL for 24 h. Following AuNS treatment, cells were washed with complete medium and incubated with fresh complete medium (100 μL) containing 10 μL MTS reagent (Sigma, UK). Cells were incubated at 37°C for 1-2 h and the optical density at 490 nm was measured to determine intracellular NADH levels. Viability was determined from the optical density as a percentage of control cells. Staurosporin was employed as a positive control for cell death. All experiments were performed in triplicate.

Lactate dehydrogenase release assay

Lactate dehydrogenase (LDH) release was used to quantify cellular membrane integrity as another parameter of AuNS biocompatibility. Following 24 h of AuNS treatment, 10 μL of cell medium were transferred to 96-well plates and mixed with 100 μL of LDH reagent (Abcam, UK) to measure the levels of released (extracellular) LDH. Cells were then lysed using the kit's cell-lysis solution (in the original incubation medium) and 10 μL of cell medium was transferred to 96-well plates and mixed with 100 μL of LDH reagent to measure total (intracellular plus extracellular) LDH. Optical density at 490 nm was measured after 5-10 mines following addition of LDH reagent, with cell viability quantified as the optical density ratio of released LDH to total LDH. Staurosporin was similarly employed as a positive control for cell death.

View Article Online
DOI: 10.1039/C8NR09409H

Transmission Electron Microscopy (TEM)

Following a 24 h treatment with 25 μg/mL AuNSs, cells were rinsed with fresh DMED culture medium and then fixed with 2.5% glutaraldehyde in 0.1M HEPES buffer, pH 7.2 for 1 h at 4°C. The fixatives were removed by washing the cells with 0.1 M HEPES buffer 3 times. Cells were scraped, transferred to 1.5 mL Eppendorf tubes and centrifuged at 1000 *g* for 20 minutes to obtain cell pellets. The cell pellets were dehydrated in graded solutions of ethanol (50%, 70%, 95%, and 100%), for 5 min x3 each, and then washed for 10 min x3 each in acetonitrile (Sigma). After dehydration, samples were progressively infiltrated with a Quetol-based resin, produced by combining 8.75 g quetol, 13.75 g nonenyl succinic anhydride, 2.5 g methyl acid anhydride, and 0.62 g benzyl dimethylamine (all from Agar Scientific). Samples were infiltrated in a 50% resin:acetonitrile solution for 2 hours, in a 75% resin:acetonitrile solution overnight and in 100% resin for 4 days, with fresh resin replaced daily. The embedded samples were cured at 60°C for 24 hours. Thin sections (90 nm) were cut from the resin blocks directly into a water bath using an ultramicrotome and a diamond knife with a wedge angle of 35°. Sections were immediately collected on bare, 300 mesh copper TEM grids (Agar Scientific), dried and stored under vacuum until TEM analysis. Bright field transmission electron microscopy (BFTEM) was carried out using a JEOL 2000 operated at 80 kV.

Results and Discussion

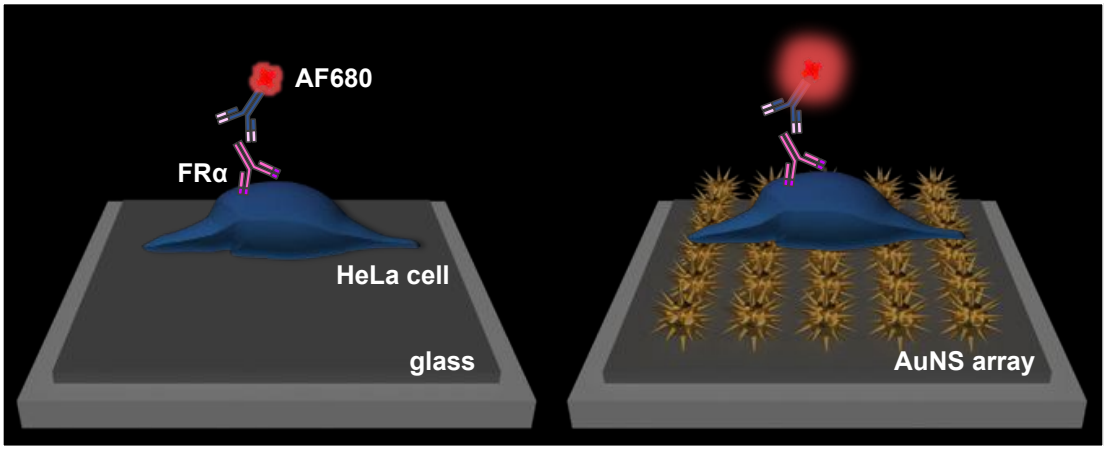

Figure 2: Schematic representation of the fluorescence-enhanced cellular assay using gold nanostar (AuNS) arrays. Compared to bare glass substrates, the plasmonic AuNS

View Article Online
DOI: 10.1039/C8NR09409H

arrays enable significant fluorescence enhancement for cellular imaging of a Folate Receptor alpha (FRα)-positive cervical cancer cell line (HeLa), labelled with a near-infrared (NIR) fluorophore (AlexaFluor® 680; AF680).

As demonstrated by our previous work, AuNS arrays are effective MEF platforms, allowing large fluorescence enhancements throughout the NIR and NIR-II biological windows for fluorophore monolayers incorporated on to the arrays.[20] Through a combination of fluorescence lifetime measurements and electric-field enhancement modelling, our findings also suggested that particle *morphology* was a crucial factor in the magnitude of electromagnetic field enhancement, and ultimately the total enhancement factor.[20] The optical properties of AuNSs are known to be highly anisotropic, strongly depending on the size of the protruding tips.[25] Finite-difference time-domain analysis has suggested that the plasmons of AuNSs result from hybridization of the core and tip plasmons of the nanostar.[18] Consequently, the ability to manipulate the morphological properties of AuNSs (*e.g.* size, number of spikes per nanoparticle, spike sharpness) enables systematic control of their plasmonic response.

Based on these findings, we expect that using AuNS arrays with tunable optical properties and morphologies, we may achieve fluorescence-enhanced NIR cellular imaging (Figure 2) with tunable enhancement factors. Therefore, AuNSs of two different sizes and geometries were synthesized through a surfactant-free seed mediated method as described in our previous work,[20] and referred to as small (S-AuNSs; Figure 3a, inset) and large (L-AuNSs; Figure 3b, inset) AuNSs. The as-synthesized colloidal S- and L-AuNSs had size distributions of 47 ± 17 nm and 214 ± 90 nm, respectively, with extinction maxima at 718 nm and 1015 nm.[20] L-AuNS comprised more spikes with sharper tips, whilst S-AuNS had relatively fewer spikes, with a lower aspect ratio and more rounded tips.[20] Unlike other plasmonic substrates previously used for fluorescence-enhanced imaging, such as gold island films,[16] this tunability of optical properties could allow AuNSs to be spectrally coupled with several different fluorophores in the NIR/NIR-II regions, which is a critical factor for determining the magnitude of MEF, as well as the development of multiplexed sensing or imaging platforms.

View Article Online
DOI: 10.1039/C8NR09409H

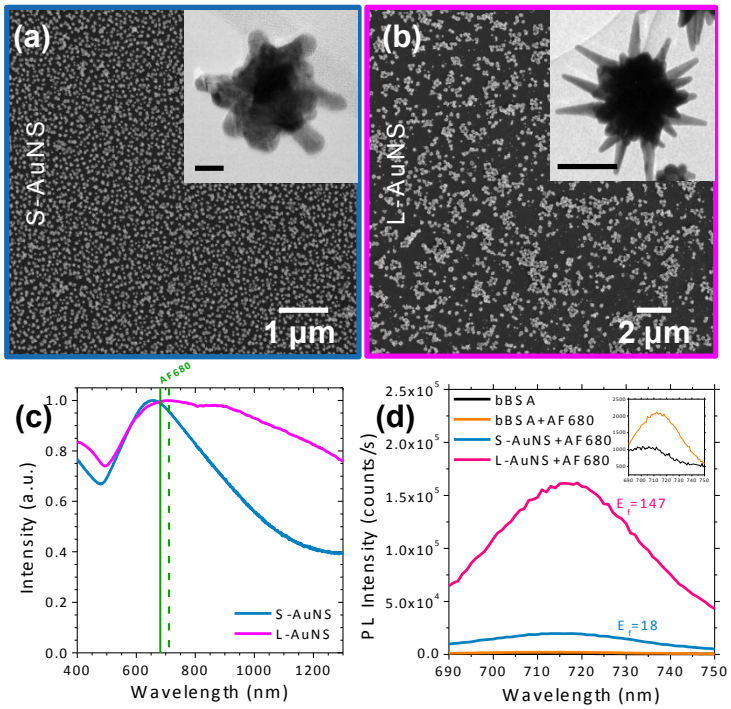

Figure 3: AuNS arrays with tunable morphologies and optical properties afford significant NIR fluorescence enhancement. (a, b) Scanning electron microscopy (SEM) images of arrays fabricated through the self-assembly of "small" (S-AuNSs) (a) and "large" gold nanostars (L-AuNSs) (b) on silanized glass slides. The insets in (a, b) are transmission electron microscopy (TEM) images of the corresponding S-AuNSs (scale bar 10 nm) and L-AuNSs (scale bar 100 nm) used for array preparation. (c) Normalized extinction spectra of the S- and L-AuNS substrates. The solid and dashed straight lines represent the excitation and emission maxima, respectively, of Alexa Fluor® 680 (AF680). (d) Photoluminescence (PL) emission spectra of monolayers of streptavidin-conjugated AF680, formed on biotinylated bovine serum albumin (bBSA)-coated glass slides and S- or L-AuNS arrays. The inset shows the PL emission of AF680 on bBSA-coated glass compared to bare (*i.e.*, in the absence of fluorophore) bBSA-coated glass slides, used for background correction.

Using the S- and L-AuNSs, plasmonic AuNS arrays were fabricated through an established procedure in our lab, based on glass silanization and AuNS self-

View Article Online
DOI: 10.1039/C8NR09409H

assembly.[20] Scanning electron microscopy (SEM) imaging revealed that the surfaces of the S -AuNS (Figure 3a) and L-AuNS (Figure 3b) arrays were densely covered by particles, with S-AuNS having a relatively more homogeneous distribution over the array surface.[20] Both AuNS arrays displayed uniform colourations over large areas (in the order of cm^2), which resembled those of the original colloidal suspensions. Therefore self-assembled monolayers of AuNSs could be formed over large areas through a straightforward procedure. This process can be easily scaled up, making it a viable option for the development of novel clinical diagnostic applications, able to delineate, for instance, between various types of cancer/healthy cells, with high specificity and sensitivity. Furthermore, the extinction spectra of the substrates, recorded directly using dry slides (Figure 3c), showed that the plasmonic AuNS arrays had tunable optical properties, throughout the first and second biological windows. For both types of substrates, there was some broadening of the optical spectra compared to those of colloidal AuNSs; according to a previous work using electromagnetic computation techniques, aggregation of AuNSs in dimers and monolayers produced widened spectral features and an increase in the magnitude of extinction.[26]

We have previously shown that similar AuNS plasmonic arrays were effective MEF platforms throughout the NIR and NIR-II regions.[20] In that work, fluorescence enhancement was measured for AlexaFluor® 750 (AF750, Abs 749 nm/Em 775 nm), AlexaFluor® 790 (AF790, Abs 782 nm/Em 805 nm) and Ag_2S quantum dots (broadband absorption, Em 1200 nm), synthesized in our lab.[7] Here, we selected a Alexa Fluor 680 (AF680, Abs 679 nm/Em 702 nm) for cell labelling during our fluorescence-enhanced cellular imaging experiments, for compatibility with our imaging system. First, we quantified the potential of the AuNS substrates for enhancing the fluorescence of AF680 molecules positioned in proximity to the AuNS surface, before using this dye for cell labelling and imaging experiments (Figure 1a). This was achieved by collecting the fluorescence emission spectra of streptavidin–functionalized AF680 monolayers deposited on to the AuNS substrates, and on bare glass substrates, as a control (Figure 3d). As previously,[20] an AlexaFluor® dye was selected because it is more hydrophobic, photostable and bright, but less pH-sensitive, compared to other commercially available dyes with similar spectral properties, making it more suitable for cell and tissue labelling.[24] Biotin-labelled bovine serum albumin (bBSA), which binds to both glass and Au surfaces,[27, 28] was used as the

View Article Online
DOI: 10.1039/C8NR09409H

spacer between glass/AuNS arrays and the fluorophore.[11] bBSA provides a spacing of ~4-8 nm between the dye molecules and the Au surface, while the streptavidin attached to the dyes, provides an additional separation distance of ~4 nm, resulting to a total spacing of ~12 nm. For the dye monolayer fluorescence enhancement experiments, the averaged fluorescence enhancement factors ($E_{f(dye)}$) of AF680 for S-AuNS and L-AuNS arrays were 18 and 147, respectively, and were calculated using:

$$E_{f(dye)} = \frac{E_{Au/dye} - E_{glass/bBSA}}{E_{glass/dye} - E_{glass/bBSA}} \cdot \frac{bBSA_{glass}}{bBSA_{Au}} \qquad (1)$$

where $E_{Au/dye}$ and $E_{glass/dye}$ is the fluorescence intensity of the fluorophore on AuNS and bare glass substrates, respectively, $E_{glass/bBSA}$ is the background fluorescence of bBSA on bare glass substrates, $bBSA_{glass}$ is the amount of bBSA bound on bare glass substrates and $bBSA_{Au}$ is the amount of bBSA bound on AuNS substrates. These enhancement factors were slightly lower than those previously measured for AF750 and AF790, in part possibly due to the higher unmodified quantum yield of AF680 (0.36), compared to the other two fluorophores (0.12 for AF750 and 0.04 for AF790).[29] Nevertheless, significant fluorescence enhancement was achieved for AF680 on both S-AuNS and L-AuNS arrays, which is several times higher than the 3-fold enhancement of a spectrally similar dye (Cy5; Abs 625nm/Em 670 nm) previously measured on gold island films,[30] and is expected to allow for substantial enhancement in cellular imaging. As anticipated, significantly larger fluorescence enhancement was achieved using the L-AuNS arrays compared to the S-AuNS. In our earlier work,[20] fluorescence lifetime measurements and analysis using a semi-empirical model for the plasmonic enhancement effects associated with fluorophores,[31] showed that the extent of emission enhancement was similar for both types of AuNS substrates. In contrast, excitation enhancement was found to be significantly higher with L-AuNS compared to S-AuNS.[20] In addition, 3D finite-difference time-domain (FDTD) modelling carried out to simulate the electric field enhancement showed drastically enhanced local field intensities around L-AuNSs compared to those of S-AuNSs.[20] Our findings therefore suggested that tuning the total fluorescent enhancement depends critically on controlling the excitation enhancement, and illustrated the significant impact of particle morphology on fluorescence enhancement.

View Article Online
DOI: 10.1039/C8NR09409H

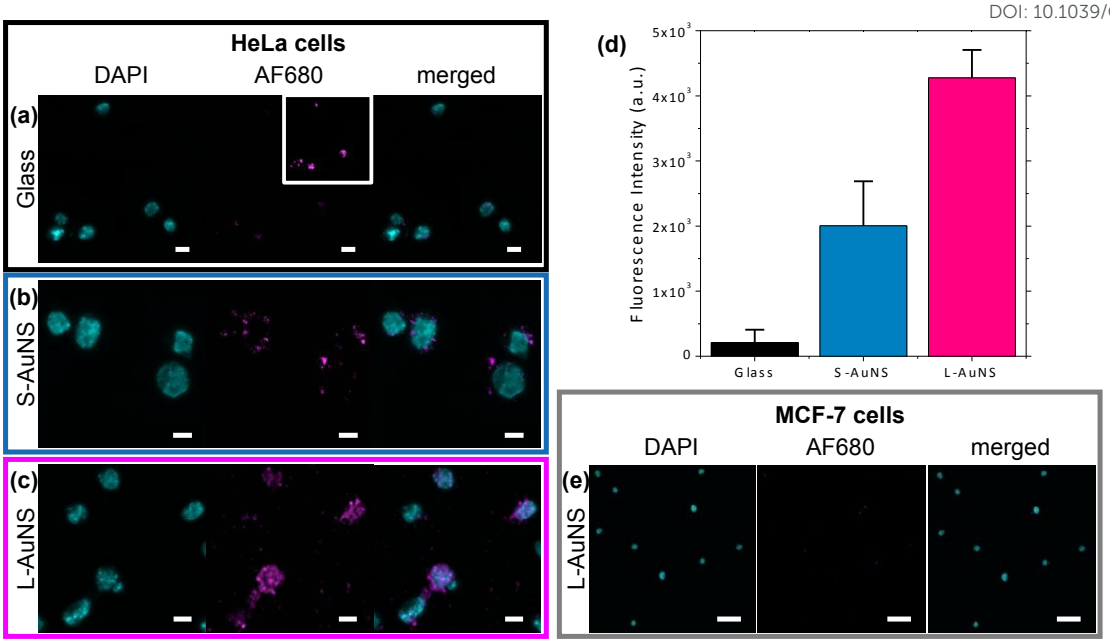

Figure 4: AuNS arrays enable tunable fluorescence enhancement for cellular imaging in the NIR biological window. (a-c) Fluorescence images of DAPI (nucleus, cyan; left) and FRα-AF680 (magenta; middle) labelled HeLa cells, and merged signals (right), on bare glass (a), S-AuNS (b) and L-AuNS (c) substrates, collected using a confocal microscope. (d) Mean fluorescence intensity (MFI) of AF680 on AuNS arrays and glass slides. The error bars represent the standard deviation of the data. (e) Fluorescence images of DAPI (nucleus, cyan; left) and FRα-AF680 (magenta; middle) labelled MCF-7 cells (FRα-negative) and merged signals (right), on L-AuNS substrates.

Having established that AuNS arrays allow for significant and tunable fluorescence enhancement of the AF680 dye, we then tested their potential under cell labelling conditions with this dye. To compare the imaging sensitivities of the two AuNS arrays, we proceeded with labelling of the Folate Receptor alpha (FRα) on HeLa cell surface using AF680, and cell imaging on the AuNS arrays, with glass slides as reference. Fixed HeLa cells were first labelled with a FRα polyclonal antibody in 5% bovine serum albumin (BSA). Cells were then washed and counterstained with an AF680-conjugated secondary antibody (donkey anti-sheep IgG AF680) in 5% BSA. After successive washing with phosphate buffered saline (PBS), around 10000 cells were adsorbed onto the AuNS substrates or bare glass slides overnight. Imaging with a confocal microscope showed that the fluorescence of

View Article Online
DOI: 10.1039/C8NR09409H

AF680 signal from individual HeLa cells on the AuNS arrays (Figure 4b, c) was higher than cells adsorbed on glass (Figure 4a). Quantification of the mean fluorescence intensity (MFI) from several cells (Figure 4d) showed that, under identical imaging conditions, the MFI of AF680-FRα labelled cells on AuNS substrates was significantly higher compared to bare glass. The enhancement factors under cell imaging conditions ($E_{f(cell)}$) were calculated by:

$$E_{f(cell)} = \frac{MFI_{AuNS}}{MFI_{glass}}$$

and were 9 and 19 times for S-AuNS and L-AuNS arrays, respectively. As a control, we used MCF-7 cells, which are FRα-negative. Fluorescence signals of AF680 from MCF-7 cells were significantly lower compared to HeLa cells on the L-AuNS arrays (Figure 4e), in accordance to their lower levels of FRα expression. The increase in MFI measured using the AuNS substrates confirms that these substrates can significantly enhance NIR fluorescence signals during cellular imaging, allowing for more sensitive detection of biomarkers. As anticipated from our fluorescence measurements of AF680 dye monolayers (Figure 3d), L-AuNS, which had been associated with higher local field intensity enhancements,[20] resulted to a higher increase in the MFI of labelled cells than S-AuNS. These findings indicate that manipulation of the electric field enhancement by controlling the geometries of plasmonic nanoparticles paves the way for sensitive cellular imaging with *tunable enhancement factors*. The ability to produce substrates with tunable enhancement factors, and therefore tune the sensitivity of detection to different concentrations of biomarkers of interest, represents a significant step forward in the development of multiplexed detection platforms. A possible limitation of our experiments may be the choice of AF680 dye, which has a short NIR emission, but was selected for compatibility with our cell imaging system. In our previous work, higher enhancement factors have been measured for dye monolayers of AF750 ($E_{f(dye)}$ up to 320 times) and AF790 ($E_{f(dye)}$ up to 195 times) deposited on AuNS substrates.[20] Therefore, further improvements in the MFI of labelled cells and the enhancement factors under cell imaging conditions ($E_{f(cell)}$) are likely if the bioplatform and imaging system are *both* optimized. For instance, under cell imaging conditions using commercially available plasmonic gold nano-island films,[16] a previous work has shown the same enhancement factors ($E_{f(cell)}$: ~30 times) for fluorescence imaging of cells labelled with either IRDye680 (which has a similar spectral response as AF680,

View Article Online
DOI: 10.1039/C8NR09409H

used in the present work) or IRDye800 (corresponding to the longest-wavelength AF790). However, the lack of systematic LSPR tuning for those commercial SPR chips,[17] compared to our AuNS arrays, may limit their potential for multiplexed applications. Our findings may open up new routes for fluorescence-enhanced cellular imaging with diminished biomolecule autofluorescence, using several ligands throughout the NIR window to simultaneously detect different cell sub-populations.

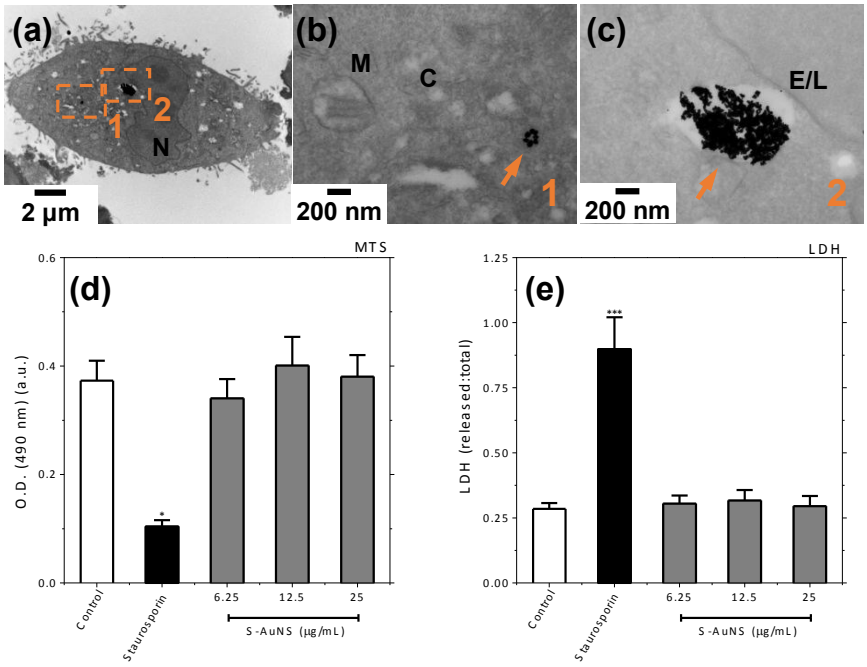

Figure 5: (a-c) TEM images of HeLa cells exposed to S-AuNSs for 24 h (N: nucleus, C: cytoplasm, M: mitochondrion E/L: endosome/lysosome). (b) and (c) are magnifications of the areas squared in (a), showing AuNS localization (arrows) in the cytoplasm or endosomal vesicles. (d) Cell viability (MTS assay; n=3) and (e) LDH release (n=3) following treatment of HeLa cells with 0-25 µg/mL S-AuNSs for 24 h. Staurosporin was used as a positive control for cell death.

Finally, to test the applicability of AuNSs for further development of *in vivo* imaging probes,[4, 32] we proceeded to test the *in vitro* uptake and biocompatibility of S-AuNSs with HeLa cells. S-AuNSs were selected, as they are significantly smaller than L-AuNSs, therefore they are expected to be more readily taken up by cells and experience more efficient clearance, making them more suitable

for *in vivo* diagnostics. Transmission electron microscopy (TEM) imaging of HeLa cells exposed to colloidal S-AuNSs for 24 h revealed that S-AuNSs had been taken up by HeLa cells (Figure 5a) and were localized in endosomal vesicles (Figure 5c) or the cytoplasm (Figure 5b), without any evidence for cell damage. Given the high biocompatibility of Au[33] and the synthesis of AuNSs through a surfactant-free protocol, which avoids the use of toxic surfactants such as CTAB, the AuNSs are expected to be highly biocompatible. HeLa cells were incubated with a dose range of 0-25 μg/mL of S-AuNSs for 24 h, using staurosporin as a positive control for cell death. Biocompatibility was assessed by a tetrazolium salts (MTS) assay and a LDH release assay, which measure the metabolic activity of cells and cell membrane permeability, respectively. Compared to the non-treated control, HeLa cell viability (Figure 5d) was not significantly changed under any exposure concentration, and no significant LDH release was measured (Figure 5e). Taken together, these results show that S-AuNSs can be effectively internalized within HeLa cells, without causing any apparent damage to cell viability, making them suitable for *in vivo* imaging. Combined with our recent work on single-particle fluorescence enhancement from NIR/NIR-II fluorophores conjugated to AuNSs via PEG spacers,[4] these findings pave the way for the development of further *in vivo* diagnostic applications.

Conclusions

In summary, plasmonic substrates based on AuNS monolayers allowed up to around 150 times fluorescence enhancement for NIR dye molecules coupled to the AuNSs. Under fluorescence cell imaging conditions, 19-fold fluorescence enhancement for NIR imaging was achieved, enabling the application of fluorescent dyes with low quantum yields for sensitive cellular imaging with low autofluorescence interference. Our findings indicate that through manipulation of the electric field enhancement around AuNSs, cellular imaging with *tunable enhancement factors* can be achieved, which will be potentially useful for the development of multicolour and multiplexed platforms. Along with AuNS uptake by HeLa cells and their biocompatibility, our results may open up new routes for novel high-performance diagnostic platforms.

Conflicts of interest

View Article Online
DOI: 10.1039/C8NR09409H

There are no conflicts to declare.

Acknowledgments

IGT and FX are supported by a British Council Newton Grant (No. 216239013). FX acknowledges an ICiC grant funded by MRC Confidence in Concept and the Royal Marsden NHS Foundation Trust. MPR is grateful for funding *via* an RAEng/Shell Research Chair in Interfacial Nanoscience. AEP acknowledges support from an ICiC confidence in Concept Grant funded by the MRC/BRC and a pump priming grant from the Rosalind Franklin Institute.

References

1. D. Darvill, A. Centeno and F. Xie, *Phys. Chem. Chem. Phys.*, 2013, **15**, 15709-15726.
2. S. Luo, E. Zhang, Y. Su, T. Cheng and C. Shi, *Biomaterials*, 2011, **32**, 7127-7138.
3. H. Wan, J. Yue, S. Zhu, T. Uno, X. Zhang, Q. Yang, K. Yu, G. Hong, J. Wang, L. Li, Z. Ma, H. Gao, Y. Zhong, J. Su, A. L. Antaris, Y. Xia, J. Luo, Y. Liang and H. Dai, *Nat. Commun.*, 2018, **9**, 1171.
4. I. G. Theodorou, Q. Jiang, L. Malms, X. Xie, R. C. Coombes, E. O. Aboagye, A. E. Porter, M. P. Ryan and F. Xie, *Nanoscale*, 2018, DOI: 10.1039/c8nr04567d.
5. R. Weissleder, *Nat. Biotech.*, 2001, **19**, 316-317.
6. S. A. Hilderbrand and R. Weissleder, *Curr. Opin. Chem. Biol.*, 2010, **14**, 71-79.
7. I. G. Theodorou, Z. A. R. Jawad, H. Qin, E. O. Aboagye, A. E. Porter, M. P. Ryan and F. Xie, *Nanoscale*, 2016, **8**, 12869-12873.
8. Z. A. R. Jawad, I. G. Theodorou, L. R. Jiao and F. Xie, *Sci. Rep.*, 2017, **7**, 14309.
9. J. Pang, I. G. Theodorou, A. Centeno, P. K. Petrov, N. M. Alford, M. P. Ryan and F. Xie, *J. Mater. Chem. C*, 2017, **5**, 917-925.
10. A. Centeno, F. Xie and N. Alford, *J. Opt. Soc. Am. B*, 2011, **28**, 325-330.

11. F. Xie, J. S. Pang, A. Centeno, M. P. Ryan, D. J. Riley and N. M. Alford, *Nano Res.*, 2013, **6**, 496-510.
12. K. Sugawa, T. Tamura, H. Tahara, D. Yamaguchi, T. Akiyama, J. Otsuki, Y. Kusaka, N. Fukuda and H. Ushijima, *ACS Nano*, 2013, **7**, 9997-10010.
13. A. Camposeo, L. Persano, R. Manco, Y. Wang, P. Del Carro, C. Zhang, Z.-Y. Li, D. Pisignano and Y. Xia, *ACS Nano*, 2015, **9**, 10047-10054.
14. B. Zhang, B. A. Pinsky, J. S. Ananta, S. Zhao, S. Arulkumar, H. Wan, M. K. Sahoo, J. Abeynayake, J. J. Waggoner, C. Hopes, M. Tang and H. Dai, *Nat. Med.*, 2017, **23**, 548-550.
15. B. Zhang, R. B. Kumar, H. Dai and B. J. Feldman, *Nat. Med.*, 2014, **20**, 948-953.
16. B. Koh, X. Li, B. Zhang, B. Yuan, Y. Lin, A. L. Antaris, H. Wan, M. Gong, J. Yang, X. Zhang, Y. Liang and H. Dai, *Small*, 2016, **12**, 457-465.
17. S. M. Tabakman, Z. Chen, H. S. Casalongue, H. Wang and H. Dai, *Small*, 2011, **7**, 499-505.
18. F. Hao, C. L. Nehl, J. H. Hafner and P. Nordlander, *Nano Lett.*, 2007, **7**, 729-732.
19. H. Yuan, C. G. Khoury, H. Hwang, C. M. Wilson, G. A. Grant and T. Vo-Dinh, *Nanotechnology*, 2012, **23**, 075102.
20. I. G. Theodorou, Z. A. R. Jawad, Q. Jiang, E. O. Aboagye, A. E. Porter, M. P. Ryan and F. Xie, *Chem. Mater.*, 2017, **29**, 6916-6926.
21. D. Feng, Y. Song, W. Shi, X. Li and H. Ma, *Anal. Chem.*, 2013, **85**, 6530-6535.
22. J. A. Ledermann, S. Canevari and T. Thigpen, *Ann. Oncol.*, 2015, **26**, 2034-2043.
23. P. Pallavicini, G. Dacarro, M. Galli and M. Patrini, *J. Colloid Interface Sci.*, 2009, **332**, 432-438.
24. N. Panchuk-Voloshina, R. P. Haugland, J. Bishop-Stewart, M. K. Bhalgat, P. J. Millard, F. Mao, W.-Y. Leung and R. P. Haugland, *J. Histochem. Cytochem.*, 1999, **47**, 1179-1188.
25. C. L. Nehl, H. Liao and J. H. Hafner, *Nano Lett.*, 2006, **6**, 683-688.
26. D. M. Solís, J. M. Taboada, F. Obelleiro, L. M. Liz-Marzán and F. J. García de Abajo, *ACS Photonics*, 2017, **4**, 329-337.

27. T. P. Gustafson, Q. Cao, S. T. Wang and M. Y. Berezin, *Chem. Commun.*, 2013, **49**, 680-682.
28. M. Borzenkov, G. Chirico, L. D'Alfonso, L. Sironi, M. Collini, E. Cabrini, G. Dacarro, C. Milanese, P. Pallavicini, A. Taglietti, C. Bernhard and F. Denat, *Langmuir*, 2015, **31**, 8081-8091.
29. J. R. Lakowicz, Y. Shen, S. D'Auria, J. Malicka, J. Fang, Z. Gryczynski and I. Gryczynski, *Anal. Biochem.*, 2002, **301**, 261-277.
30. S. M. Tabakman, L. Lau, J. T. Robinson, J. Price, S. P. Sherlock, H. Wang, B. Zhang, Z. Chen, S. Tangsombatvisit, J. A. Jarrell, P. J. Utz and H. Dai, *Nat. Commun.*, 2011, **2**, 466.
31. A. I. Dragan and C. D. Geddes, *Appl. Phys. Lett.*, 2012, **100**, 093115.
32. L. Y. Chou and W. C. Chan, *Adv. Healthcare Mater.*, 2012, **1**, 714-721.
33. R. Shukla, V. Bansal, M. Chaudhary, A. Basu, R. R. Bhonde and M. Sastry, *Langmuir*, 2005, **21**, 10644-10654.

TOC entry

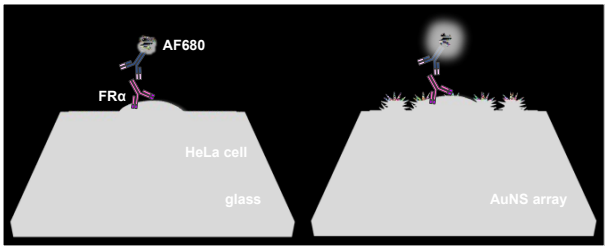

Gold nanostars increase the brightness of weakly-emitting dyes in the near-infrared biological window for cellular imaging with tunable enhancement factors.